2023

Deformation analysis in the surroundings of the roadway ahead of longwall mining, Staszic-Wujek mine, Poland

Petr Waclawik
Czech Academy of Sciences

Radovan Kukutsch
Czech Academy of Sciences

Kristyna Schuchova
Czech Academy of Sciences

Jan Nemcik
University of Wollongong, jnemcik@uow.edu.au

Andrzej Walentek
Central Mining Institute Poland

See next page for additional authors

DEFORMATION ANALYSIS IN THE SURROUNDINGS OF THE ROADWAY AHEAD OF LONGWALL MINING, STASZIC-WUJEK MINE, POLAND

Petr Waclawik[1,*], Radovan Kukutsch[1], Kristyna Schuchova[1], Jan Nemcik[2], Andrzej Walentek[3], Aleksander Wrana[3], Sahendra Ram[4] and Jiri Korbel[5]

ABSTRACT: Accurate knowledge of the stress-strain state in rock mass is absolutely critical to optimise support design. Therefore, the rock mass stresses are often measured for reasons of safety and efficiency in underground mining. Investigation of the rock mass stress is usually carried out by interpretation of the rock mass deformation processes. These can be monitored and measured. The compact conical-ended borehole overcoring (CCBO) probe was used to measure the pre-mining full stress tensor and afterwards three compact conical-ended borehole monitoring (CCBM) probes were installed to continuously monitor stress changes in rock mass ahead of the advancing longwall II/501/C mining seam 501 in the Staszic-Wujek coal mine in Poland. The purpose of the monitoring was to quantify changes in stress tensor during the mining process. At the monitoring site the extracted seam had an average thickness of 3.4 m at a depth of about 890 m and lies within the Polish part of the Upper Silesian Coal Basin. The maximum measured stress of 30 MPa was oriented close to horizontal and amost parallel to the monitored roadway. The deformation analysis of roadway was carried out using a pulse 3D laser scanner at the geotechnical station. Due to favourable orientation of the lateral stress, the deformation changes in the roadway surroundings the monitoring station were minimal.

INTRODUCTION

The knowledge of stress state in rock mass (RM) is very important in mining geomechanics. Generally, the accurate knowledge of the stress strain state of the RM in the neighbourhood of the mining galleries and underground openings is absolutely critical for their optimum support design not only in the vicinity of them, but also at a greater distance away. Measurement (investigation) of the rock stress is usually carried out by interpretation of the RM deformation processes, which can be relatively precisely observed and measured.

To measure initial in situ stress in RM, the Compact Conical ended Borehole Overcoring (CCBO) method was used. The CCBO probes were developed at the Institute of Geonics in cooperation with University Kumamoto. K.Sugawara and Y. Obara (Sugawara and Obara 1999, Obara and Sugawara 2003) were the first who developed and used the compact conical-ended borehole overcoring system. To measure stress changes in the state of stress in the RM, the Compact Conical ended Borehole Monitoring method (CCBM) (Stas et al. 2005, 2011) was used. This method is based on the principles of the modified overcoring method. The measurement probe is glued directly to the conical top of installation hole to monitor continuously changes in stress that occur in RM during mining processes.

The stress state monitoring in Staszic-Wujek coal mine was designed for one geotechnical monitoring station in the entry roadway of the longwall with the power loader technology. The geotechnical station was located in the entry roadway No. II/501/C at the chainage of 296 m from the longwall face. The CCBM probes were installed at the end of February, 6 weeks before the start of longwall mining. Exploratory hole was drilled before installation to determine the positions of probes with respect to the lithological development within the RM. The geotechnical station was designed within the technical limits of the maximum length and incline of the installation holes.

1 Dr./Researcher, Institute of Geonics, the Czech Academy of Sciences, Czech Republic (*) Corresponding author: petr.waclawik@ugn.cas.cz
2 Dr./ Honorary Senior Fellow, University of Wollongong, Australia
3 Dr./Researcher, Central Mining Institute, Poland
4 Dr./Assistant Professor, National Institute of Technology Rourkela, India¨
5 Head of the Operation of Mining Safety Services, CSM Mine, OKD Company, Czech Republic

The deformation analysis of roadway at the monitoring station was carried out using a pulse 3D laser scanner. The purpose was to capture deformation changes ahead of the advancing longwall face; specifically, at five stages in the ± 20 m section on each side from the GS.

METHODOLOGY OF MEASUREMENT

Methodology of initial in situ stress measurement

The CCBO method is an in situ measurement of stress relief in the RM. It uses the inherent behaviour of the rock core due to overcoring process. Overcoring itself causes the rock-core stress release, which is manifested by a deformation response. The relationships between the measured strains along the perimeter of the probe provide the ability to calculate the stress state in which the rock was initially placed (Stas et al. 2007a,b, 2011). The CCBO probe is a conical-shaped device that allows determination of the full stress tensor of the rock from only one borehole measurement (Waclawik et al. 2016). The strains in the tangential and radial directions are measured through strain gauges located at the probe surface (**Figure 1**). The original probe design, which contained eight strain gauge rosettes (Sugawara and Obara 1999), was modified to use only six strain gauge rosettes (Fig. 1).

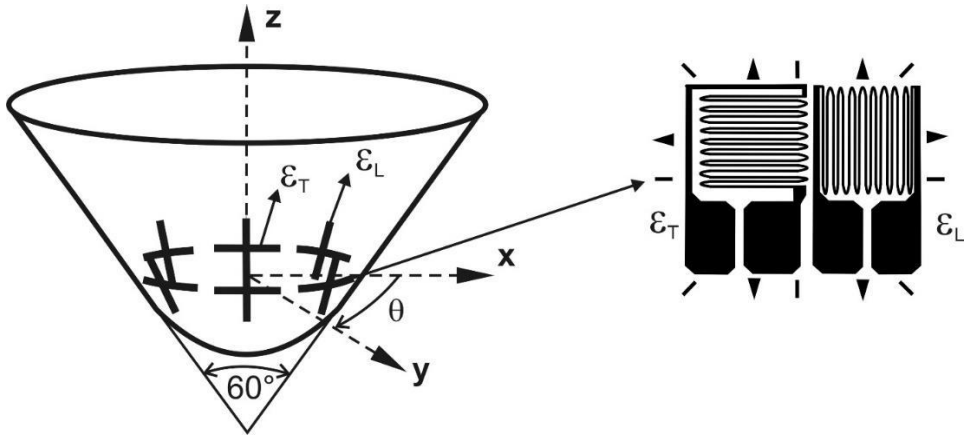

Figure 1: Geometry of CCBO probe (Waclawik et al. 2016)

The conical shape of the probe's surface has the advantage of measuring the stress tensor in one position and simple installation and centering of the probe strain gauges. Relatively short compact segment of rock is required for application of this overcoring method.

Dependence of corresponding gauge sensor (Nakamura 1999, Stas et al. 2004, Stas et al. 2008) is formulated by:

$$\varepsilon\Delta^{\Phi j} * E = | A(\Delta;\Phi_j) | * |\sigma|$$

where: $\varepsilon_\Delta{}^{\Phi j}$ - calculated deformation on gauge sensor of Δ type ($\Delta \in \{T,L\}$) and Φ_j adjusted to x-axis ($j \in \{1,\ldots\ldots m\}$, m-number of sensors); E – Young´s modulus; | A($\Delta;\Phi_j$) | is 6-elements row matrix; the elements depend on Δ type and Φ_j orientation of corresponding gauge sensor; $|\sigma|$ - stress tensor represented by column matrix ($|\sigma|^T=\{\sigma_{xx}, \sigma_{yy}, \sigma_{zz}, \sigma_{xy}, \sigma_{xz}, \sigma_{yz}\}$). Optimal stress tensor $|\sigma|$ of the system is found by method of least squares of differences of the corresponding measured $\varepsilon_{\Delta\Phi j}$ and calculated $\varepsilon_\Delta{}^{\Phi j}$ deformations.

The CCBO probe is designed for holes 76 mm in diameter. The waterproof probe body has a diameter of 55 mm. Six pairs of mutually perpendicular strain gauges are mounted onto the conical tip of the probe with an apical angle of 60°.

Methodology of stress state changes monitoring of rock mass

The CCBM method is based on similar principles as the CCBO method except for the 'destructive' overcoring phase which is not performed. This method allows a repeated measurement of strain on all sensors of the probe over a long period. In this case, however, only changes of the stress tensor in relation to the stress state at the time of probe installation (i.e. to the reference state) can be determined.

This is the principal difference between the CCBO and CCBM methods. The evaluation of measurements remains the same as in the case of the CCBO technique.

The dependence of corresponding deformations on the tensometers on the stress tensor was formulated by Sugawara and Obara (1999) and Obara and Sugawara (2003). For the CCBM, the following equation was formulated (Stas et al 2011):

$$[\varepsilon_{\wedge}^{\Phi j}(t_i) + \varepsilon_{\wedge}^{\Phi j}(\Delta t)] \times E = |\boldsymbol{A}(\Lambda;\mu;\Phi_j)| \times [\,|\boldsymbol{\sigma}_i| + |\boldsymbol{S}(\Delta t)|\,]$$

and the following was expressed using it:

$$\varepsilon_{\wedge}^{\Phi j}(\Delta t) \times E = |\boldsymbol{A}(\Lambda;\mu;\Phi_j)| \times |\boldsymbol{S}(\Delta t)|,$$

where $\varepsilon_{\wedge}^{\Phi j}(t_i)$ and $\varepsilon_{\wedge}^{\Phi j}(\Delta t)$ are the deformation $\varepsilon_{\wedge}^{\Phi j}$ at the time of the installation of the probe and the differential deformations related to the time of installation; $|\boldsymbol{\sigma}_i|$, $|\boldsymbol{S}(\Delta t)|$ are the tensors at the time of installation t_i and the induced stress tensor (stress changes at the time Δt after installation) related to the stress state $|\boldsymbol{\sigma}_i|$; E is Young's modulus and μ is Poisson's ratio. The optimum stress change tensor of the whole system can be calculated using the differences of all ("j-") pairs of the corresponding measurements ($\varepsilon_{\wedge}^{\Phi j}(\Delta t)$) and the ideal expected deformation ($\varepsilon_{\wedge\Phi j}(\Delta t) \equiv |\boldsymbol{A}(\Lambda;\mu;\Phi_j)| \times |\boldsymbol{S}(\Delta t)|/E$) can be calculated using the method of least squares.

The CCBM probe is designed for holes 76 mm in diameter. The waterproof probe body has a diameter of 55 mm. Six trio of strain gauges are mounted onto the conical tip of the probe with apical angle of 60° at the level where the diameter is 38 mm. The probe is glued directly in the conical shaped bottom of the hole. The CCBM probe, which can be connected to an external control unit by cable, thus enables the observation of stress changes in the rock mass (induced, for example, by underground mining activities). Periodic manual reading of data was carried out by Personal Digital Assistant (PDA). The data concerning stress changes in CCBM probes were read minimally three times per week with only minor exceptions (technical problems with the reading device or oxidation of cable contacts).

Methodology of measurement of roadway deformations

Within scanning the longwall roadway, Faro Focus S 350 scanner was used (see **Figure 2**). This is a device with a long laser beam range, which is distinguished by its spatial, length and angle accuracies and its high scanning rate. The subject of scanning work was scanning longwall roadway No. II/501/C under the longwall, using the power loader technology. Similar verification of stress state monitoring in the surroundings of the roadway ahead of longwall mining based on the results of 3D scanning of roadway deformation was discussed for Bogdanka and CSM Mine (Kukutsch et al. 2016, Waclawik et al. 2022). The GS was installed in the roadway concerned in the surroundings of which scanning works took place. The purpose was to capture deformation changes ahead of the advancing longwall face; specifically, in five steps in the ± 20 m section on each side of the GS. The subject of the first step was the initial scanning at the time of longwall face start for the purpose of capturing the current state; additional steps were scanning this station at distances of 285, 198.5, 165, 119.5 and 91.5 m in front of the longwall face with the already possible detection of space-time changes. Scanning closer to the longwall face was not allowed for the safety reasons.

With regard to the minimum blocking of the operational time in the roadway concerned such resolution was selected that enables to capture the roadway in sufficient detail, nevertheless respecting and considering mining operation. The chosen resolution was 1/4 (the detail level for the inside spaces up to max. 10 m to the point of interest) in quality 2x (43.7 million. points within one position). Scanning itself with this resolution, including the time for setting the tripod, took 4-5 minutes at each station. With regard to the high humidity and temperature, scanning itself was preceded by waiting for approx. 30 minutes to equalise temperature of the scanner optics to prevent water vapours condensation on the surface of the rotating glass. The specified step between individual stations was 5 m, i.e. such distance that ensures the optimum coverage of the mine work from two consecutive stations. A necessary activity within 3D laser scanning is the registration of partial point clouds to create one unit. A condition of every successful registration is the detection of at least a pair of joint detection points (reference spheres and targets) within at least a pair of connected partial point clouds. To ensure that the processing and registration of partial scans are as precise as possible, reference spheres with a diameter of 140 mm and checkerboard targets with 20 x 20 cm size were used. When they were used, the achieved middle

distance errors (registration errors) were in the order of up to 3 mm. A condition for problem-free registration is not only the visibility of the ground control points from one and more stations but also respecting the conditions for setting the reference balls resulting from the chosen resolution. For the purpose of aligning clouds, the reference balls had a fixed stated position (the reflective label on the reinforcement specifying unmistakebly their position) at the border of the selected section to enable alignment of the mutual point clouds. The details of all scanning campaigns are given in **Table 1**.

Figure 2: Scanning of the longwall roadway by Faro Focus S 350 scanner

Table 1: Overview of the scanning campaigns at the geotechnical station, *automatically generated cloud to cloud error from the TRW

Date	Distance to longwall	Number of positions	Registration error	Number of captured points	Length of the captured section
20. 04. 2022	285.0 m	6	1.21 mm	727,175,158	34 m
26. 05. 2022	198.5 m	8	1.92 mm	1,049,828,771	42 m
22. 06. 2022	165.0 m	7	1.30 mm	892,830,273	38 m
14. 07. 2022	119.5 m	8	2.93 mm	1,050,110,493	37 m
28. 07. 2022	91.5 m	8	3.10 mm	1,051,622,829	38 m

Scan registration itself took place in fully automated mode in the case of using reference balls. All captured partial point clouds were successfully connected to create one unit defined by the general united coordinate system based on the position of the scanner within one of the partial stations. The output of subsequent data processing in the Trimble Realworks (TRW) software is a continuous cloud of spatial points (hereinafter referred to as a “cloud”), describing in detail the scanned space. The results of partial scan registration are shown in **Figure 3.**

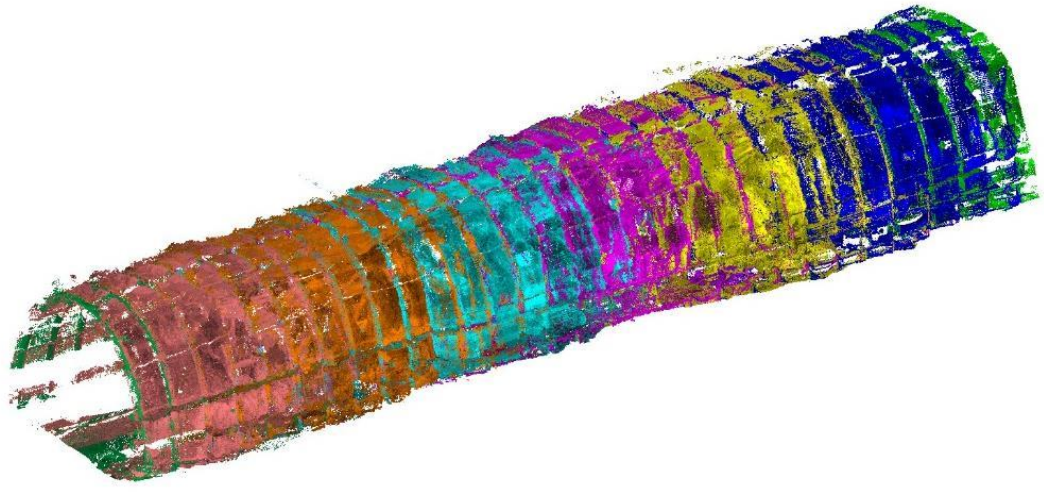

Figure 3: The section of roadway No. II/501/C in the surroundings of the geotechnical station

An additional task following scan registration was to clean a point cloud so that the point cloud has no elements that complicate the mutual alignment of clouds. All visible mine technologies (conveyor belt, suspension track locomotive and others), cables, mine workers, and the like were removed to ensure that only the roadway floor ground, sides and roof remain. The clouds cleaned in this way were compared with each other. A difference scan will then enable to show the places and sizes of the captured deformation changes.

Determination of deformation and mechanical properties of rocks

Deformation and mechanical properties of rocks have a significant influence on rock deformation characteristic during stress measurement process by CCBO and CCBM probes. Texture and composition of each rock type determine these properties. It is necessary to know deformation and mechanical properties of rocks for correct determination of stress state in RM. In order to obtain the information about the qualitative parameters of rocks, the basic deformation and mechanical properties of rocks were studied. In particular, the bulk density ρ0 the uniaxial compressive strength (UCS) σ_D, Young's modulus E, and Poisson's ratio μ were defined. The methodologies of determination of deformation and mechanical properties were based on common technical norms (EN 1926) and ISRM (International Society for Rock Mechanics) recommendations (Bieniawski and Bernede 1979 a,b).

Standard laboratory device equipment was used to determine deformation and mechanical properties. The compressive strengths and deformation properties of rocks were tested using the ZWICK 1494 mechanical press machine with the special load cell using the LVDT (Linear Variable Displacement Transformer) sensor. Four sensors were used to measure longitudinal deformation and eight to measure transversal deformation (see **Figure 4**). The compressive test was carried out at the loading rate of about 0.15 mm/min.

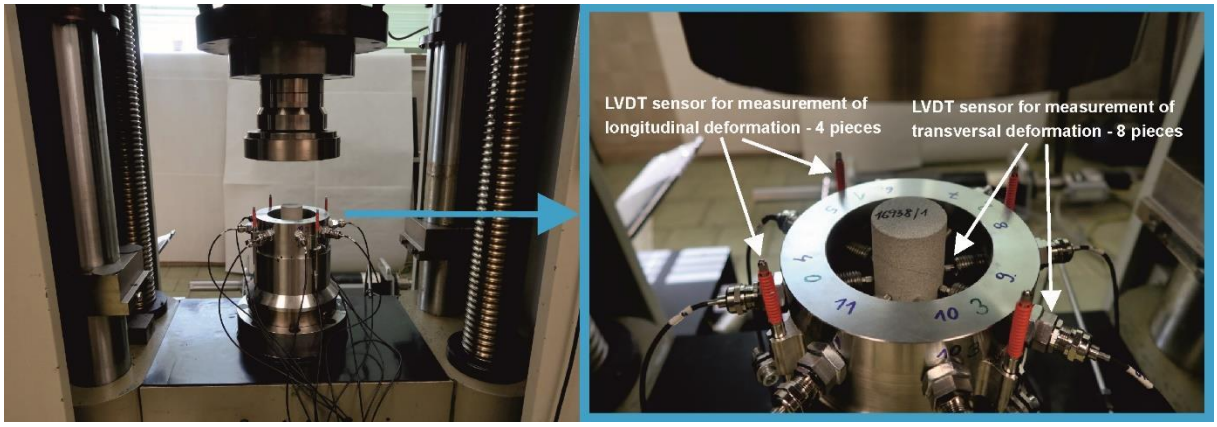

Figure 4: Mechanical press machine with load cell

DESIGN OF ROCK MASS STRESS CHANGES MEASUREMENT AHEAD OF PANEL II/501/C

The monitoring of the stress changes of the RM ahead the II/501/C panel face was designed as one monitoring station with a location in roadway II/501/C in the station chainage of 296 m from longwall face (see **Figure 5**). In order to monitor the stress changes of the RM due to longwall II/501/C advance, three holes were used. Three CCBM probes in total were placed in such a way that they monitored independently the stress state of the rock mass ahead of the longwall face of longwall II/501/C (CCBM1, electronics No. 2, CCBM 2, electronics no. 3 and CCBM 3, electronics no. 4). The location of the CCBM and CCBO probes are shown in **Figure 6**. The layout was designed with respect to the technical limits of installation, limiting the maximum length of the installation hole and its incline.

Longwall II/501/C, using the power loader technology, was situated at a depth of approximately 890 m under the surface. The bedding of the seam is sub-horizontal. The strata dip oriented in the SSW, direction is 7°. Exceptionally, the localised dip of the coal seam can reach up to 10°. Thickness of the seam varied from 3.05 m up to 3.65 m. Average thickness of the longwall No. II/501/C is about 3.4 m.

From the geomechanical point of view, the RM is formed with varied range of rock material and variable physical-mechanical properties. The lithological sequence is complicated because the river sedimentation markedly influenced the sedimentary process. The lithology was verified by upper

exploratory hole T1 20 m in length at the projected location of GS. The lithological sequence in the vicinity of the coal seam No. 501 is presented in **Figure 6**. In the area of the influence there are no extracted longwalls and in the rock cover above the longwall no exploitation was carried out in the past.

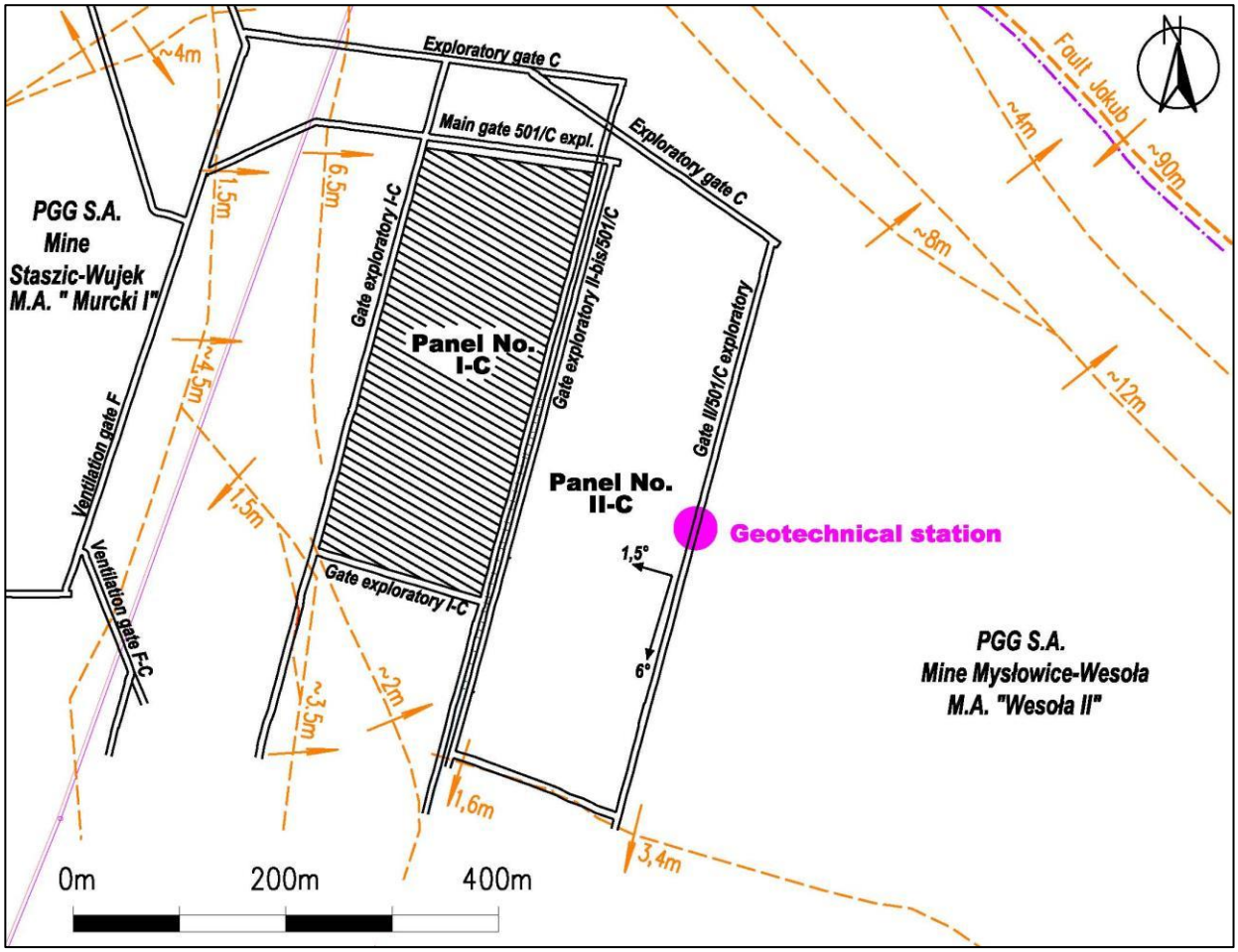

Figure 5: Location of geotechnical station GS in relation to longwall II/501/C

On the basis of the lithological development and other RM parameters, the installation holes were designed and location of the conical probes were selected. CCBM1, CCBO1 and CCBM2 probes were installed in the siltstone, while the CCBM3 probe was installed in the sandstone. To install the CCBM and CCBO probes, three installation holes 76 mm in diameter were drilled. Only the last two meters of these installation holes were cored to obtain samples necessary for the determination of the physical and mechanical properties. The parameters of the installation holes are shown in **Table 2**.

Table 2: Parameters of the installation holes and CCBM(O) probes installed in roadway II/501/C

Probe No.	Stationing [m]	Hole direction	Hole No.	Hole incline	Probe depth [m]	Electronics number	Date of installation
CCBO 1	291.7	70°	1	+38°	15.2	-	9.2.2022
CCBM 1	291.8	70°	1	+38°	16.0	2	10.2.2022
CCBM 2	296.3	75°	2	+58°	12.5	3	17.2. 2022
CCBM 3	286.6	60°	3	+19°	15.6	48	28.2. 2022

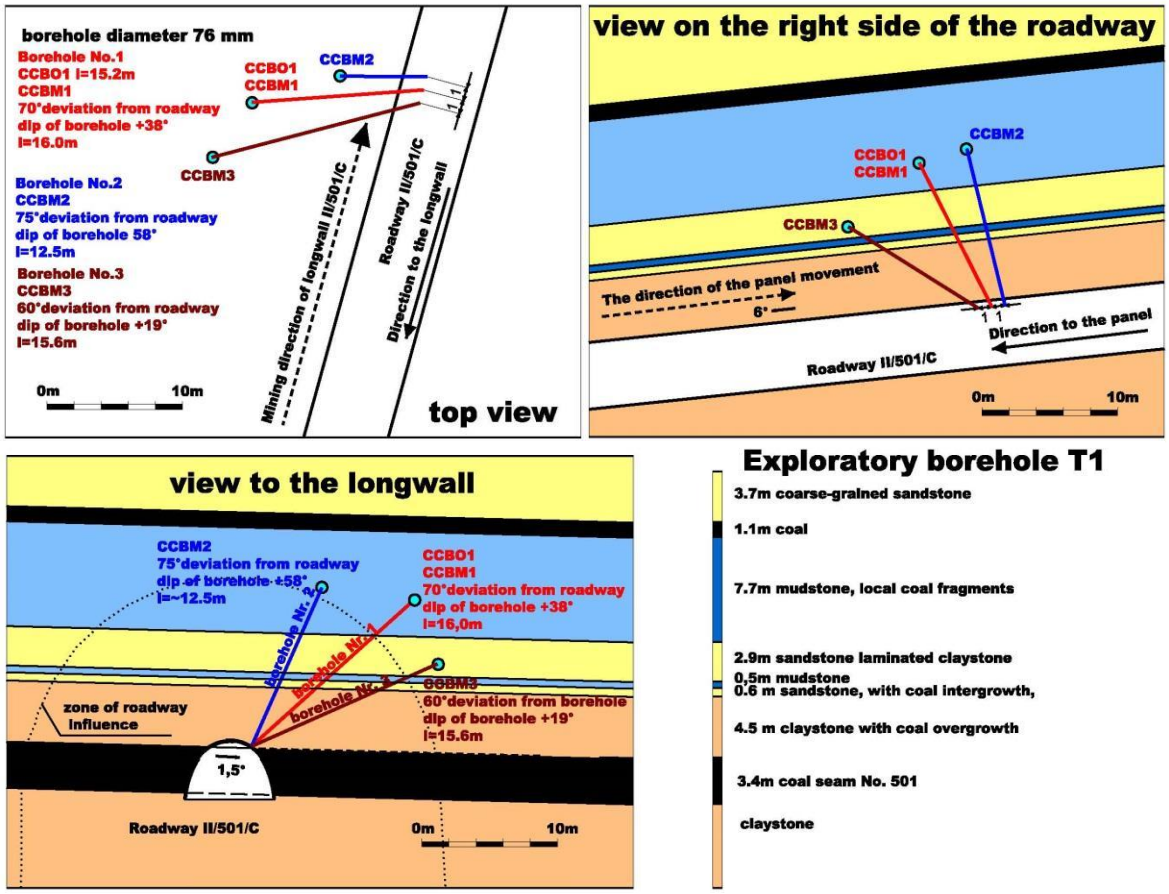

Figure 6: Positions of the CCBM(O) probes and installation holes in relation to roadway II/501/C

RESULTS AND DISCUSSIONS

Assessment of deformation and mechanical properties of rock

The evaluated results are shown in **Table 3**. Cylindrical samples with the length-to-diameter ratio (slenderness ratio) about 2:1 (61 mm in diameter, 121 mm high) were used to determine these basic properties. Bulk density was calculated from the sample dimensions and weight of the sample. Example of typical stress-strain diagrams (sample No. 17 181/3) is presented in **Figure 7**. The typical failure characteristic (sample No. 17 181/3) is shown in **Figure 8**.

Table 3: Bulk density ρ_0, UCS σ_D, Young's modulus E, Poisson´s ratio υ of rocks tested

Sample No.	Diam.[mm]	High [mm]	ρ_0 [kg/m^3]	σ_D [MPa]	E [MPa]	μ [-]	Rock type	Borehole No./depth [m]
17 181/1	61.29	121.00	2627	59.1	25 045	0.20	siltstone	1/15.2
17 181/2	61.17	120.84	2627	48.7	27 034	0.13	siltstone	1/15.4
17 181/3	61.27	121.16	2727	57.6	31 301	0.19	siltstone	1/15.6
17 181/4	61.27	121.02	2618	43.5	24 373	0.15	siltstone	1/15.8
17 181/7	61.22	121.33	2633	57.0	22 178	0.23	siltstone	2/12
17 181/8	61.11	121.34	2647	82.7	20 590	0.15	siltstone	2/11.8
17 181/9	61.17	121.46	2636	42.3	17 214	0.29	siltstone	2/11.6
Average value	61.23	121.16	2640	53.3	23 067	0.19	-	-
Deviation	0.06	0.19	35.3	13.6	4 604	0.05	-	-
Coef. of var.[%]	0.1	0.2	1.3	25.5	20.0	27.6	-	-

Using the known strength classifications of intact rocks (for an overview, see Bieniawski 1989), the intact samples of siltstone taken from the installation boreholes can be classified as „moderate strong“ to „strong“ rocks. According to another classification of Hoek and Brown (1997), the siltstone tested in

terms of the average value of UCS (53 MPa) measured on the intact samples also belong to the group of „strong“ rocks, being placed at the lower limit of this category, i.e. at the transition to the group of „medium strong“ rocks.

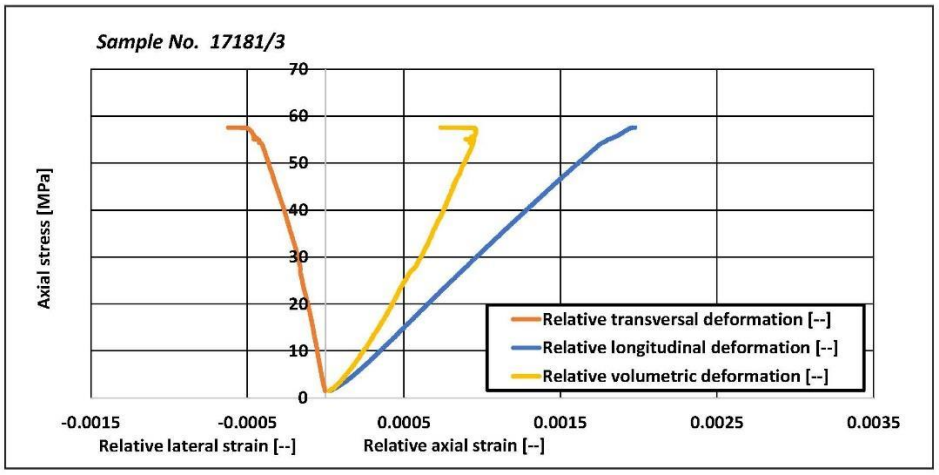

Figure 7: Example of working diagram of the uniaxial compressive strength determination test

Figure 8: Typical failure characteristic of testing sample (left before test, right after test)

Due to the fact that the installation boreholes were inclined to the bedding foliation (borehole No. 1 +38°, Borehole No. 2 +58°), the results of deformation and mechanical properties are influenced or rather reduced (e.g. Khanlari et al. 2014). The failure characteristics of all tested rock samples are similar, as the bedding foliations were the predisposing surface for failure (see **Figure 8**).

The following deformation and mechanical properties were determined for probe CCBM1, which was installed in borehole No. 1: σ_D = 52 MPa , E = 26.9 GPa, and μ = 0.17. Rock sample No. 17181/5 was not considered due to the occurrence of a crack in the original sample. The following deformation and mechanical properties were determined for probe CCBM2, which was installed in borehole No. 2: σ_D = 61 MPa, E = 20.0 GPa, and μ = 0.22. The deformation and mechanical properties for the CCBO probe were determined from rock sample Nos. 17181/2 a 17181/3: σ_D = 53 MPa , E = 29.2 GPa, and μ = 0.16.

Assessment of initial stress tensor

Hole drilling, overcoring (using CCBO) and installation of CCBM probes were completed before starting the longwall excavation. The locality of monitoring of the stress state and stress changes, including spatial orientation (see **Figure 6**), were described in the previous chapter. Total stress tensor was detected using the overcoring CCBO method in installation borehole No. 1. The overcoring process was successful with 100 % percent core recovery (see **Figure 9**).

Interpreted principal stress values are shown in **Table 4** and in **Figure 11**. If we consider the theoretical value of gravitational stress of about 21 MPa (for the depth of 890 m below surface), then it is evident

that the indicated values do not correspond to the theoretical idea of distribution of stress fields. It has become apparent that the stress distribution is influenced by the geological properties. As mentioned above, the determined deformation and mechanical properties were influenced by the orientation of the bedding foliation in relation to the compressive loading in mechanical press machine. In the case of a CCBO probe which was installed in a borehole with inclination +38°, the deformation and mechanical properties can be reduced by up to 30% (see **Figure 10**). Given that the deformations of the RM caused by overcoring process are recalculated on the basis of knowledge of the deformation and mechanical properties, this factor is essential. It is important, that the proportions of stress components and their orientation are not affected by this factor. Assessed magnitudes and spatial orientation of principal stress components are given in **Table 4**.

Figure 9: Core recovery from overcoring

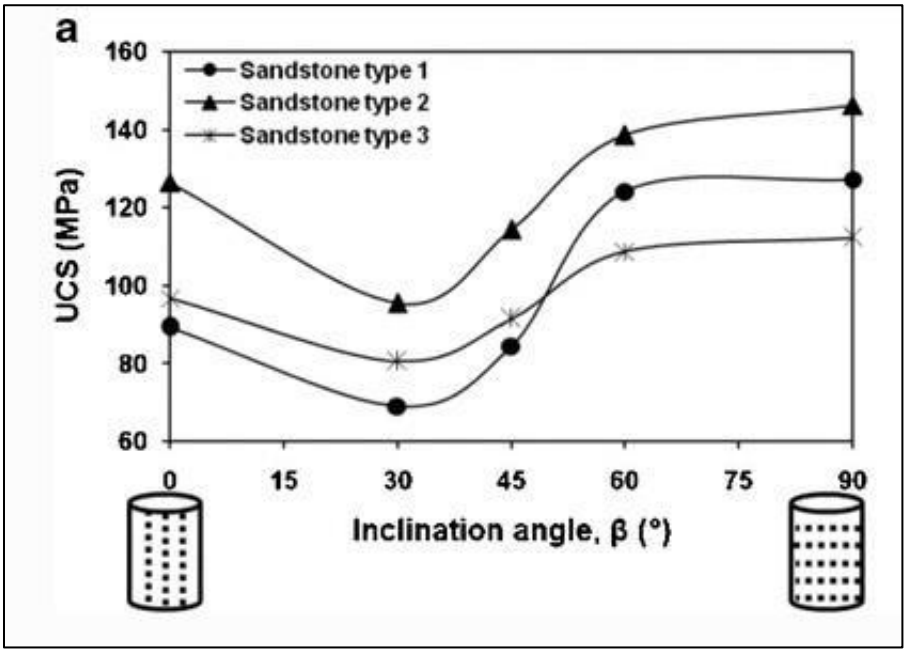

Figure 10: Influence of orientation sedimentary foliation to UCS value (Khanlari et al. 2014)

Table 4: Values of principal stress components and their spatial orientation (CCBO)

Maximum stress - S1	Dip of axis	Dip direction of axis	Medium stress - S2	Dip of axis	Dip direction of axis	Minimum stress - S3	Dip of axis	Dip direction of axis
33.5 MPa	-27°	357°	22.2 MPa	-34°	247°	2.9 MPa	-44°	116°

The results of the spatial distribution of all stress tensors from the overcored CCBO probe are presented in Fig. 19a. In the figure, the directions of principal stress components are depicted using the stereographic projection in the lower hemisphere. The maximum stress component axis is presented as a ring, the medium stress component axis as a square and the minimum stress component axis as a triangle.

Horizontal stresses, their magnitudes and directions are significant features of the stress distribution in the vicinity of the roadway. That is why they were analysed in the course of our experiment.Their directions and magnitudes projected onto the horizontal plane are shown in **Figure 11**. S_H means the maximum horizontal stress and S_h means the minimum horizontal stress.

The calculated vertical stress value Sv (15.2 MPa) interpreted from the probe CCBO was influenced by rock deformation and mechanical properties (see above). It is significant that the magnitude of the

maximum horizontal S_H component is twice the magnitude of the vertical stress component (vertical stress of 15.2 MPa). Thus, the previously observed trend from Czech part of the Upper Sillesian Coal Basin (USCB) that the maximum stress is predominant in the horizontal plane (Waclawik et al. 2018, 2019, 2020), has been confirmed.

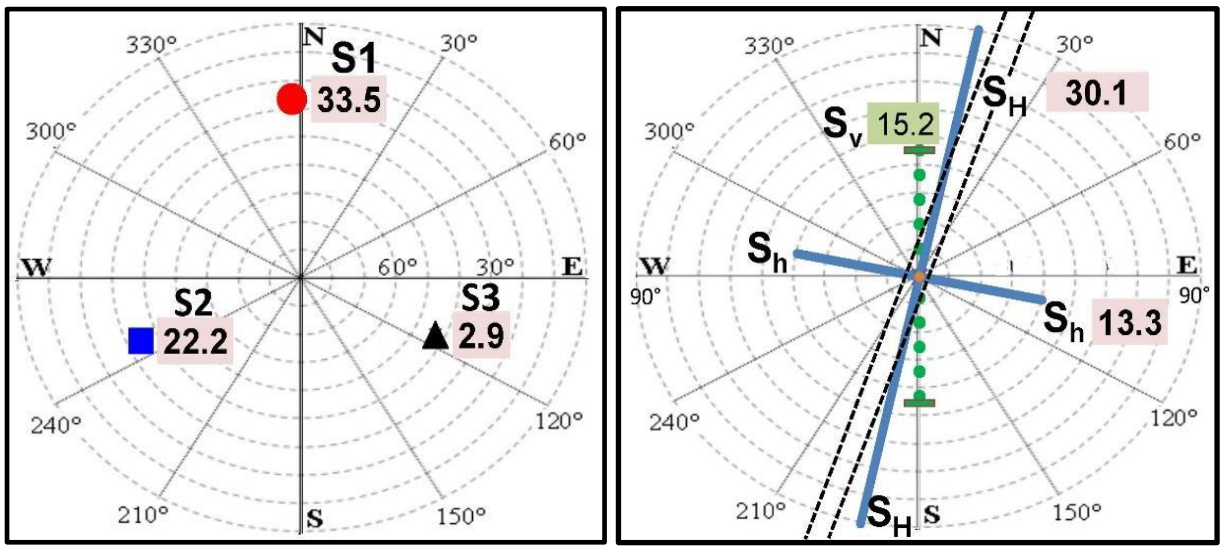

Figure 11: Spatial orientation of principal stress components calculated from CCBO probe (left) and directions of horizontal stresses (right) calculated from CCBO probe (black double dashed line represents direction of roadway No. II/501/C)

The significance of the effect of the maximum horizontal stress component S_H was also confirmed by the observed borehole breakout. These borehole breakouts in the direction perpendicular to the direction of the maximum stress were recorded during the video inspection of exploratory borehole T1 and the installation boreholes No.1 and 2 at the monitored location (see **Figure 12**).

Figure 12: Example of breakouts at the exploratory borehole T1 and installation borehole No. 1

The trend of significantly greater maximum horizontal stress (S_H) compared to vertical stress (S_v) has been confirmed in several world coal basins and also in the Czech part USCB. This trend was also confirmed in the Mine Staszic-Wujek, where the measured maximum horizontal stress component S_H is approximately 2 times higher than the vertical stress S_v. To minimise the damage to mine roadways, orientation of the roadways and longwall gateroads should be close to the direction of the maximum horizontal stress (S_H).

Monitoring of stress changes ahead of longwall face

Longwall mining started on 5st April 2022 while now, all stress probes are situated in the goaf area of the longwall and stress changes monitoring is completed. Stress changes on CCBM probes (CCBM1 and CCBM2) ahead of the advanced longwall face are presented here. The CCBM3 probe failed due to technical damage in the initial monitoring stage. The measured stress changes (stress tensor components of Sigma 1, Sigma 2 and Sigma 3) ahead of the longwall face advancing towards the probes

CCBM 1 (electronic No. 2) and CCBM 2 (electronic No. 3) are documented in **Figures 13** and **14**. Stress tensor components are graphically distinguished.

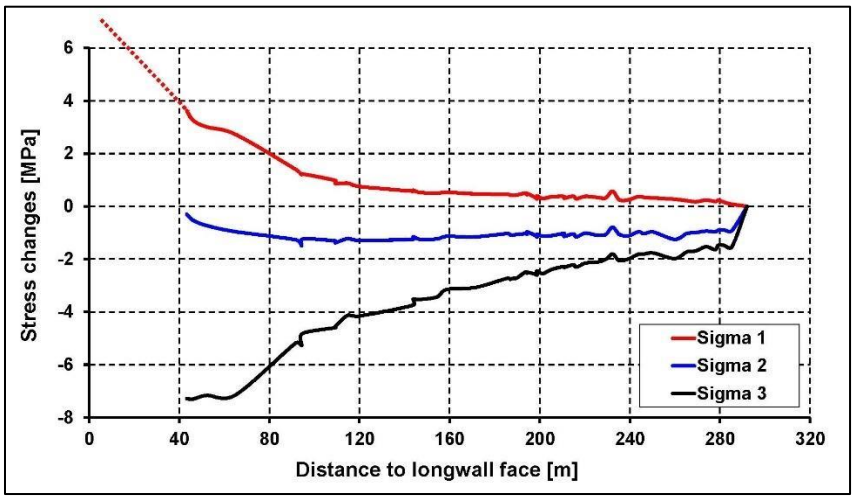

Figure 13: Changes in the stress tensor components (Sigma 1 – maximum, Sigma 2 – medium and Sigma 3 minimum) depending on the distance from the edge of the longwall face (probe CCBM 1)

Dependence of stress changes (Sigma 1, Sigma 2 and Sigma 3) on distance to the longwall face (II/501/C) measured on the CCBM1 probe is depicted in **Figure 13**.

This probe was installed into the siltstone roof over the mined area of the longwall (see **Figure 6**). Increase of significant stress changes started 90 m ahead of the longwall face as shown in the graph **(Figure 13**). The minimum stress component Sigma 3 gradually relieved to -7.3 MPa at 43 m ahead of the longwall face. The medium stress component of Sigma 2 relief was slightly more than -1 MPa and approached -0,5 MPa at location 43 m ahead of the face. The maximum stress component of Sigma 1 increased and it reached its maximum (3.7 MPa) at the distance 43 m from the longwall face (24th August 2022). Unfortunately, the monitoring of this probe could not continue because the power supply cable of probe CCBM1 was damaged. Repairs of the power supply cable were not allowed for mining safety reasons.

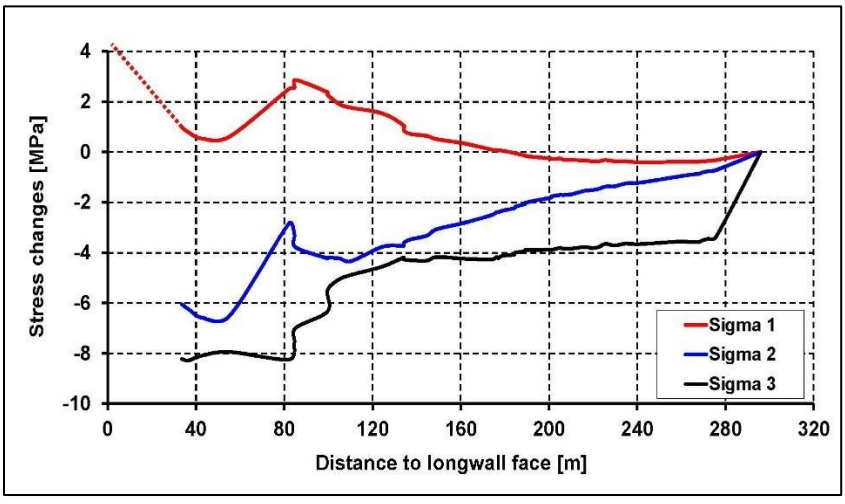

Figure 14: Changes in the stress tensor components (Sigma 1 – maximum, Sigma 2 – medium and Sigma 3 minimum) depending on the distance from the edge of the longwall face (probe CCBM 2)

Dependence of stress changes (Sigma 1, Sigma 2 and Sigma 3) on distance to the longwall face (II/501/C) measured on the CCBM2 probe is depicted in **Figure 14**. This probe was installed into the

siltstone roof over the mined area of the longwall (see **Figure 6**). Increase of significant stress changes started at the distance 95 m from the longwall face as shown in the graph (**Figure 14**). The minimum stress component of Sigma 3 gradually relieved reading -8 MPa when 82 m ahead of the longwall face where it remained at that value until 34 m from the face. The medium stress component of Sigma 2 also measured stress relief of -4 MPa when 85 m ahead of the face. Further relief of approximately 6 MPa was observed until 34 m from the longwall face. The maximum stress component of Sigma 1 increased by 3 MPa when 85 m ahead of the face. At that distance of approximately 85 m from the longwall face (25th July 2022), there was a rapid drop in all stress components. This decrease is related to the stoppage of the longwall due to geological problems experienced in the previous week (see **Figure 15**). The maximum stress component of Sigma 1 again increased from 18th August (distance longwall face – CCBM2 probe at 55 m). Subsequently, the maximum stress component of Sigma 1 increased and reached 1 MPa at distance 43 m from the longwall face (24th August 2022). The power supply cables of CCBM2 probe was also damaged, as in the case CCBM1 probe. Repair of the power supply cable were not allowed due to mining safety reasons.

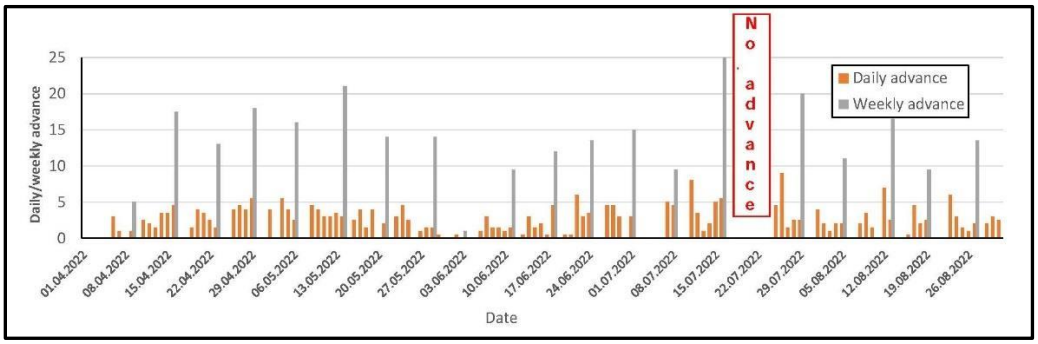

Figure 15: Daily and weekly advance of longwall face II/501/C

Deformation analysis by 3D laser scanning

As already described above, scanning of roadway No. II/501/C took place in 5 campaigns on 20/04/2022, 26/05/2022, 22/06/2022, 14/07/2022 and 28/07/2022. From the viewpoint of the distance from the longwall, point clouds were compared with each other at distances of 285 m, 198.5 m, 165 m, 119.5 and 91.5 m from the longwall. Mutual comparisons can be seen in **Figures 16 to 20.**

Figure 16 shows that no changes have occurred and the changes detected in dark blue (0.0001 – 0.03 m) represent the unchanged state. The deformations of the steel arch reinforcement are not visible. The green colour detects changes in cables, pipes.

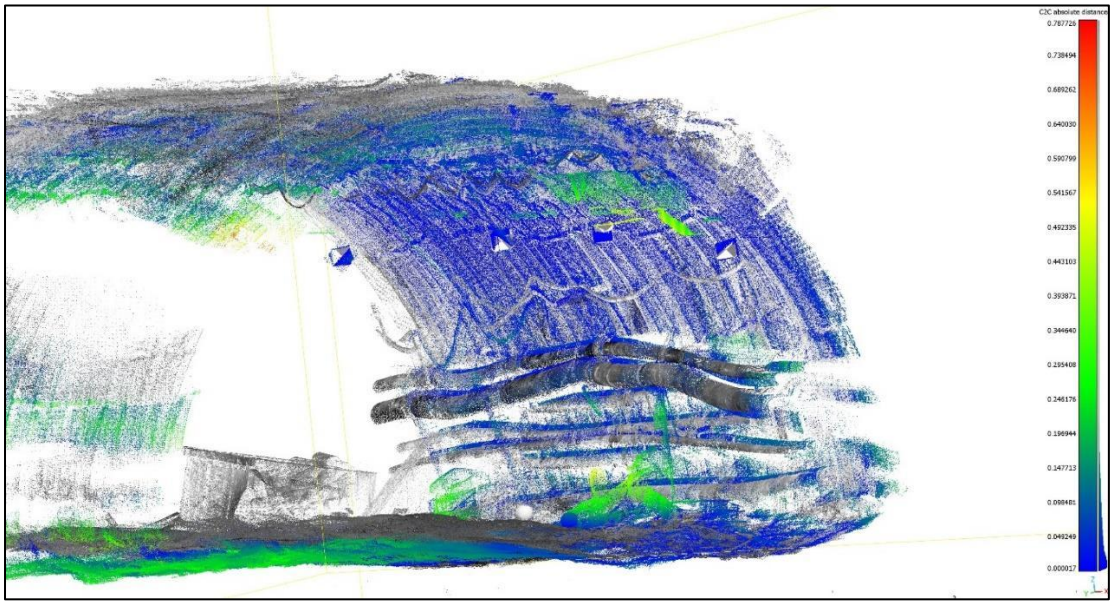

Figure 16: View of the geotechnical station; comparison of changes 285 m x 198.5 m ahead from the longwall face

The scaned data in **Figure 17** show that there have been no significant changes to the reinforcement, the blue colour still represents minimal changes in range (0.0001 – 0.05 m). On the contrary, changes from 0.5 m and more are represented by green to red colour (1 m), but these are devices that were imported into the corridor (boxes, pipes, etc.).

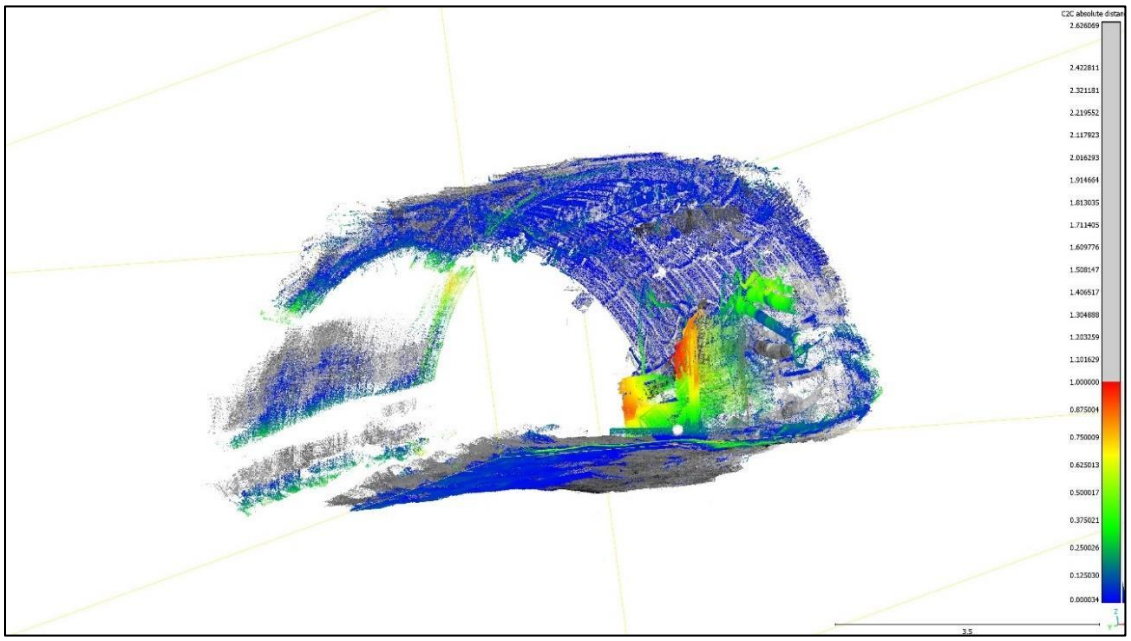

Figure 17: View of the geotechnical station; comparison of changes 198.5 m x 165m ahead from the longwall face

In this comparison in **Figure 18**, there are noticeable changes characterising the changes in the view of the transport of material to the longwall, small, gradual changes in the reinforcement begin on the pillar side. However, the green and yellow colours are not representative, as they are places not scanned (blocking the laser beam by the ventilation pipe).

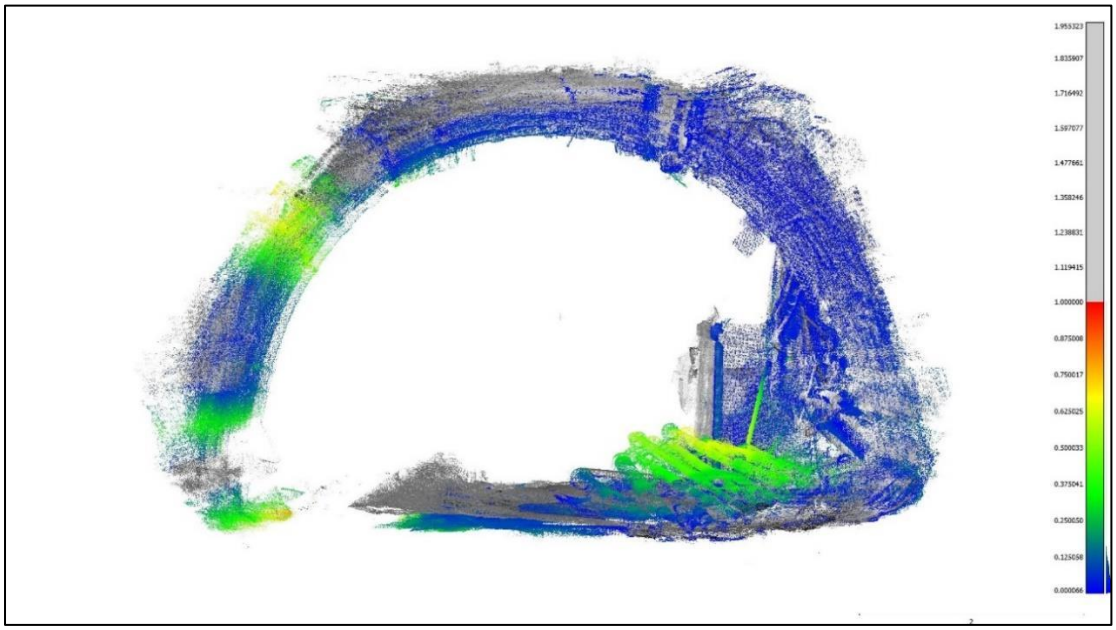

Figure 18: View of geotechnical station; comparison of changes 165 m x 119.5 m ahead from the longwall face

Figure 19 represents the beginning of floor heave, as well as the movement on the pillar side of the roadway. The pillar side of the roadway, which was already more visible at the time of scanning than in

previous campaigns, also enters the comparison, which is already better, but not optimal. Changes 0-5 cm are in blue colour while the green colour changes represent 15 cm of movement.

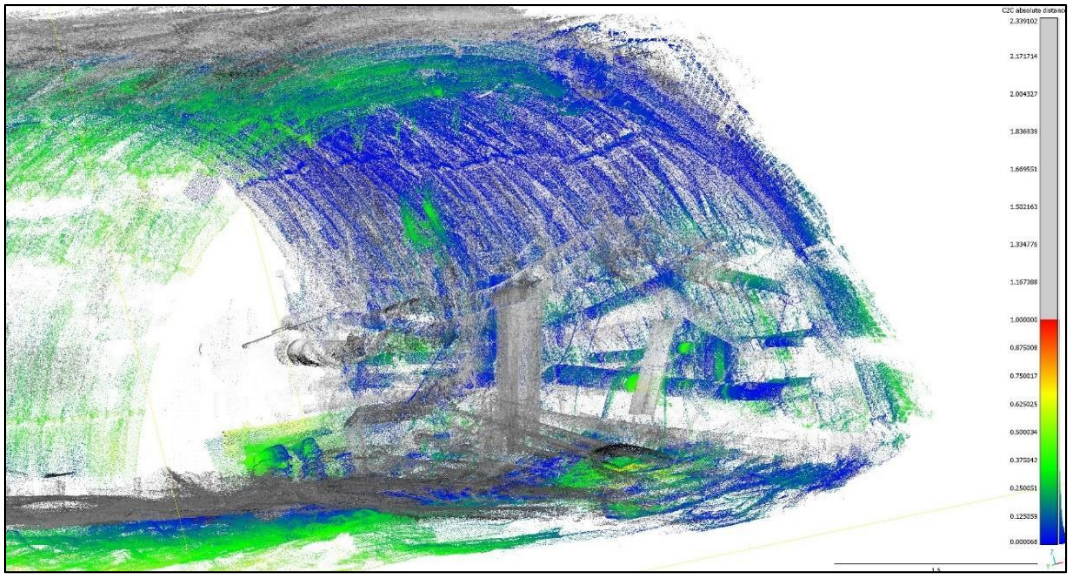

Figure 19: View of the geotechnical station, comparison of changes 119.5 m x 91.5 m ahead from the longwall face

Figure 20 represents the detected changes within the comparison of the 1st and 5th campaigns, i.e. distances of 285 m and 91.5 m from the longwall face. The blue colour here represents changes of 0-12 cm, the green colour represents changes of 20-40 cm. These changes are particularly noticeable on the pillared side of the rodway. The yellow colour is not a reference colour, because the sections length was different (34 x 38 m). In general, it can be stated that the first changes are by no means large as detected at the time when the longwall was located approx. 90 m from the GS, which correspond with deformation monitored by CCBM1 a CCBM2 probes.

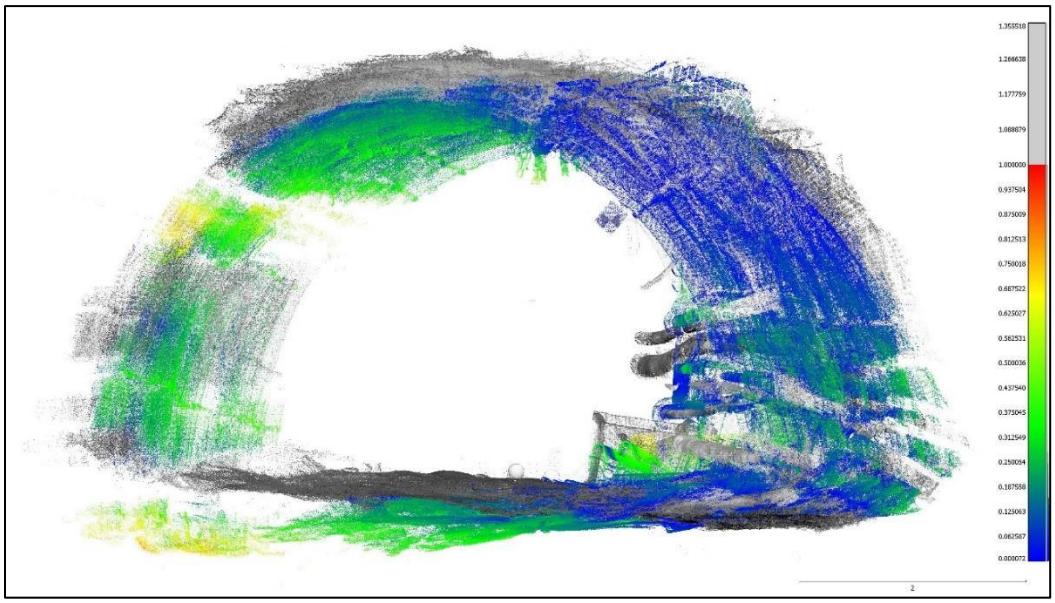

Figure 20: View of the geotechnical station, comparison of changes 285 m x 91.5 m ahead from the longwall

SUMMARY AND CONCLUSIONS

The objective of the stress monitoring carried out in the forefield of the coalface No. II/501/C was to verify the original state of the rock mass stress tensor and to study stress changes during the coal seam

exploitation. In this case, stress changes in rock can be expected due to stress re-distribution ahead of the the longwall face.

The theoretical vertical stress at a depth of 890 m, where the primary rock stress measurement was carried out, was calculated to be approximately 21 MPa. The interpreted rock vertical stress (Sv) of 15.2 MPa from the CCBO probe was affected by orientation of bedding foliation to the direction of loading axis during compressive test of rock samples. In the case of a CCBO probe which was installed in a borehole with inclination +38°, the deformation and mechanical properties were reduced up to 30%. The magnitude of the maximum component of the horizontal stress (S_H) is significant. The maximum horizontal stress component S_H (30 MPa) is approximately 2 times higher than the observed vertical stress Sv (15.2 MPa). The previously observed trend that the maximum stress value is caused in the almost horizontal plane was thus confirmed.

The expected changes in the rock stress caused by the strata loading ahead of the longwall face were recorded by the CCBM monitoring probes. Based on the evaluation of CCBM probe, the increase of significant stress changes started at the distance of 85 - 90 m from the longwall face. The development of stress change components monitored by the CCBM probes correspond to the experience of stress changes ahead of the longwall face during the longwall mining in the Carboniferous rock mass of Czech part of the USCB.

According to the pulse 3D scanner displacement measurements, we can state that the deformation changes are particularly noticeable on the pillar side of the roadway. In general, it can be said that the first deformation changes are by no means large as detected at the time when the longwall was located 90 m from the geotechnical station. These findings correspond to the measured direction of the main horizontal stress S_H, which is almost parallel to the mine roadway II/501/C. The favourable roadway direction resulted in observed better roadway conditions.

ACKNOWLEDGEMENT

This article was supported by a project DD-MET (co-financed by European Union under GA no. 847338-DD-MET and Polish Ministry of Science and Higher Education 5073/FBWiS/19/2020/2) and a project for the long-term conceptual development of research organizations (RVO: 68145535).

REFERENCES

Bieniawski, Z.T., 1989. Engineering rock mass classifications: a complete manual for engineers and geologists in mining, civil and petroleum engineering. John Wiley & Sons, Inc., New York, 251 pp.

EN 1926. Natural stress test methods – Determination of uniaxial compressive strength. European Committee for Standartization, 2006, 19 pp.

Bieniawski, Z.T., Bernede, M.J., 1979a. Suggested methods for determining the uniaxial compressive strength and deformability of rock materials: Part 1. Suggested method for determination of the uniaxial compressive strength of rock materials. - International Journal of Rock Mechanics and Mining Sciences & Geomechanics Abstracts, 16, 2, pp. 137-138.

Bieniawski, Z.T., Bernede, M.J. 1979b. Suggested methods for determining the uniaxial compressive strength and deformability of rock materials: Part 2. Suggested method for determining deformability of rock materials in uniaxial compression. - International Journal of Rock Mechanics and Mining Sciences & Geomechanics Abstracts, 16, 2, pp. 138-140.

Hoek, E., Brown, E.T., 1997. Practical estimates of rock mass strength. International Journal of Rock Mechanics and Mining Sciences, 34, 8, 1165-1186.

Khanlari G., Rafiei B., Adilor Y., 2014. Evaluation of strength anisotropy and failure modes of laminated sandstones. Arabian Journal of Geosciences. 8, 3089-3102.

Kukutsch, R, Kajzar, V, Waclawik, P and Nemcik, J, 2016. Use of 3D laser scanner technology to monitor coal pillar deformation, in Proceedings of the 2016 Coal Operators´ Conference. Wollongong: The University of Wollongong, 2016 - (Aziz, N.; Kininmonth, B.), pp 109-117. https://ro.uow.edu.au/coal/598/

Obara, Y., Sugawara, K., 2003. Updating the use of the CCBO cell in Japan: overcoring case studies. International Journal of Rock Mechanics and Mining Sciences, 40, 7-8, 1189-1203.

Sugawara, K., Obara, Y., 1999. Draft ISRM suggested method for in-situ stress measurement using the compact conical – ended borehole overcoring (CCBO) technique. International Journal of Rock Mechanics and Mining Sciences, 36, 3, 307-322.

Stas, L., Soucek, K., Knejzlik, L., Waclawik, P., Palla, L., 2011. Measurement of Stress Changes Using a Compact Conical- Ended Borehole Monitoring. Geotechnical Testing Journal, 34, 6, 685-693.

Stas, L., Knejzlik, J., Rambousky, Z., 2005. Conical strain gauge probes for stress measurement, In Proceedigs of Eurock 2005 - Impact of Human Activity on the Geological Environment, Leiden: A.A.Balkema Publishers, pp. 587-592.

Stas, L, Soucek, K, Knejzlik, J., 2007a. Conical borehole strain gauge probe applied to induced rock stress changes measurement. In 12th International Congress on Energy and Mineral Resources. Proceedings, pp. 507-516.

Stas, L., Soucek, K., Knejzlik, L., 2007b. First results of conical borehole strain gauge probes applied to induced rock mass stress changes measurement. Acta Geodynamica et Geomaterialia, Vol. 4, No. 4, pp. 77-82.

Waclawik, P., Stas, L., Nemcik, J., Konicek, P., Kalab, T., 2016. Determination of stress state in rock mass using strain gauge probes CCBO, Procedia Engineering, 149, pp. 544-552.

Waclawik, P., Kukutsch, R., Nemcik, J., 2018. Assessment of coal pillar stability at great depth. Proceedings of the 18th Coal Operators' Conference, Mining Engineering, University of Wollongong, pp. 184-194, https://ro.uow.edu.au/coal/698/

Waclawik, P., Ram, S., Kumar, A., Kukutsch, R., Mirek, A., Nemcik, J., 2019. Field and simulation study for rock bolt loading characteristics under high stress condition. Proceedings of the 2019 Coal Operators Conference, Mining Engineering, University of Wollongong,, pp. 171-179. https://ro.uow.edu.au/coal/734

Waclawik, P., Nemcik, J., Kukutsch, R., Gong, L., Venticinque, G., 2020. Dynamic events at longwall face, CSM Mine, Czech Republic. Proceedings of the 2020 Coal Operators' Conference, University of Wollongong - Mining Engineering, pp. 233-241. https://ro.uow.edu.au/coal/776/

Waclawik, P., Kukutsch, R., Walentek, A., Herezy, L., Schuchova, K., Korbel, J., 2022. Verification of stress state monitoring in the surroundings of the roadway ahead of longwall mining based on the results of 3D scanning of roadway deformation, Bogdanka Mine, Poland. Proceedings of the 2022 Resource Operators Conference, University of Wollongong - Mining Engineering, University of Southern Queensland, pp. 164-176. https://ro.uow.edu.au/coal/846/